

UR-1452  
DTP/96/08  
hep-ph/9605369  
May 1996

# Soft Gluon Radiation in Top Events: Effect of Hadronic $W$ Decays

Bond Masuda, Lynne H. Orr

*Department of Physics, University of Rochester  
Rochester, NY 14627-0171, USA*

and

W.J. Stirling

*Departments of Physics and Mathematical Sciences, University of Durham  
Durham DH1 3LE, England*

## Abstract

In reconstructing the top quark momentum from its decay products, one must account for extra jets that can result from radiation of gluons. In this paper we study soft gluon radiation in top production and decay at the Fermilab Tevatron. We consider the cases where one or both  $W$  bosons decays hadronically, *i.e.*, where at least one of the top quarks can be fully reconstructed. We show results for gluon distributions at the Tevatron and find that radiation from the  $W$  decay products contributes substantially in the central region.

# 1 Introduction

The top quark's existence is now well established [1, 2] and top searches have given way to top studies. In measuring the top quark's properties — in particular, its mass — radiated gluons can play an important role. This is due not only to the relatively high probability that  $t\bar{t}$  events are accompanied by additional gluon jets, but also to the fact that gluons can be radiated in both the top production and decay processes. This can complicate top momentum reconstruction, leading to ambiguities in identifying the top quark's decay products, increased systematic uncertainties, or both. These effects in turn influence any measurement based on momentum reconstruction, and may also bias event selection based on identifying top events via invariant mass cuts. Therefore it is necessary to understand the distributions of radiated gluons in top quark events.

There have been a number of studies of gluon radiation in top quark production and decay at  $e^+e^-$  [3, 4, 5, 6, 7] and  $p\bar{p}$  colliders [7, 8, 9, 10, 11, 12]. In [9] we examined additional gluons in the processes  $q\bar{q}, gg \rightarrow bW^+\bar{b}W^-$  at the Tevatron  $p\bar{p}$  collider in the soft gluon approximation and in [11] we performed the exact calculation. These studies included all effects of gluons radiated from the initial state partons, from the  $t$  and  $\bar{t}$  quarks at the production stage, and from the  $t$  and  $b$  (and  $\bar{t}$  and  $\bar{b}$ ) in the  $t \rightarrow bW$  decay; all effects of the width in the top propagator were also included. These studies did *not* include gluon radiation from hadronically decaying  $W$  bosons, so that, strictly speaking, they are directly applicable only to dilepton events, in which both  $W$ 's decay leptonically. But in the most useful channel — ‘lepton + jets’ — only one of the  $W$ 's decays leptonically, and the other decays to quarks. The presence of one charged lepton in this channel helps suppress backgrounds without sacrificing event rate, while jets from the hadronic  $W$  decay allow for direct reconstruction of one of the top quarks' decay products. These events can also be accompanied by extra gluons. In fact they are more likely to do so than dilepton events, because there are more colored particles available to radiate.

In this paper we extend the study of Ref. [9] for radiation of soft gluons in top production and decay at the Tevatron to include gluon radiation in hadronic  $W$  decays,  $W \rightarrow q\bar{q}'$ . In the next section we present analytic expressions for all contributions to the gluon radiation probability in the soft gluon approximation, with a discussion of properties of the  $W$  decay piece. In section 3, we apply the results of section 2 to  $t\bar{t}$  production and decay at the Tevatron and show the resulting gluon distributions. Expectations for the LHC are briefly discussed. Section 4 contains our conclusions.

## 2 Soft gluon radiation in $t\bar{t}$ production and decay: general formalism

At leading order,  $t\bar{t}$  production and decay is given by the subprocess(es)

$$a(k_1) + b(k_2) \rightarrow t(q_1) + \bar{t}(q_2) \rightarrow b(p_1) + W^+ + \bar{b}(p_2) + W^- , \quad (1)$$

where  $ab = q\bar{q}$  or  $gg$  for hadron colliders, and the particles' momenta are indicated in parentheses. Let us assume that the  $W^+$  decays hadronically:

$$W^+ \rightarrow q(p_3) + \bar{q}'(p_4). \quad (2)$$

If we are interested in the all jets case, then both  $W$ 's decay hadronically and we also have

$$W^- \rightarrow q'(p_5) + \bar{q}(p_6). \quad (3)$$

Now consider emission of a gluon with momentum  $k^\mu$ . It can come from any of the quarks or gluons in the above processes (*i.e.*, any of the particles whose momenta are labeled). This includes initial state radiation, gluons emitted by the top (or  $\bar{t}$ ) quark in either the production or decay process,<sup>1</sup> and gluons emitted by the daughter quarks of the  $t$  and  $\bar{t}$  and the  $W$  boson(s).

Because of the infra-red divergence associated with radiation of gluons, an extra jet in a  $t\bar{t}$  event will usually be soft. In the limit of soft gluon emission, several simplifications occur. First, the gluon momentum  $k^\mu$  does not affect the kinematics, so that all of the leading-order kinematic relations still hold.<sup>2</sup> Second, the differential cross section factorizes into the lowest-order cross section multiplied by a gluon radiation probability; following [4, 8, 9] we can write

$$\frac{1}{d\sigma_0} \frac{d\sigma}{dE_g d\cos\theta_g d\phi_g} = \frac{\alpha_s}{4\pi^2} E_g \mathcal{F} , \quad (4)$$

where  $d\sigma_0$  is the differential cross section for the lowest-order process (*i.e.*, with no gluon radiation),  $E_g$  is the energy of the soft gluon, and  $\alpha_s$  is the strong coupling. The function  $\mathcal{F}$  is the sum of ‘antenna patterns’ of the radiation from the different sources listed above. It can be written generically as

$$\mathcal{F} = \mathcal{F}_{\text{PROD}} + \mathcal{F}_{\text{DEC}} + \mathcal{F}_{\text{INT}} \quad (5)$$

---

<sup>1</sup>Gluons emitted by the top quark in the production and decay processes do not involve separate Feynman diagrams; integrating over the  $t$  quark's virtuality picks up poles corresponding, respectively, to emission in the two stages. See [4] for a discussion.

<sup>2</sup>While this makes the computations simpler, it also means that results of the soft calculation cannot be used to study the details of top mass reconstruction, which requires an exact treatment.

where  $\mathcal{F}_{\text{PROD}}$  is the contribution from emission at the  $t\bar{t}$  production stage (including initial-state radiation),  $\mathcal{F}_{\text{DEC}}$  is the contribution from emission off the  $t$  and  $\bar{t}$  and their decay products at the weak decay stage, and  $\mathcal{F}_{\text{INT}}$  is the contribution from interferences between these emissions. Because we are interested in hadronic  $W$  decays, it is useful to further decompose  $\mathcal{F}_{\text{DEC}}$  explicitly into the contribution from radiation off the  $t$ 's and  $b$ 's, and that from radiation off the quarks from the  $W$  decay(s):

$$\mathcal{F}_{\text{DEC}} = \mathcal{F}_{\text{DEC,tb}} + \mathcal{F}_{\text{DEC,W}}. \quad (6)$$

$\mathcal{F}_{\text{DEC,W}}$  includes contributions from one or both  $W$  decays as appropriate.

The interference term  $\mathcal{F}_{\text{INT}}$  contains contributions from the interference (i) between radiation in the  $t$  decay and that in the  $\bar{t}$  decay and (ii) between radiation in  $t\bar{t}$  production and radiation in either decay. (As discussed below, there is no contribution to the interference from the  $W$  decays because the  $W$  boson is a color singlet.) In principle  $\mathcal{F}_{\text{INT}}$  can have substantial effects for gluon energies comparable to the top decay width  $\Gamma_t$  [4, 5]. However, the observable soft jets that are relevant to the  $p\bar{p}$  collider experiments have energies much larger than  $\Gamma_t$ , and so in practice the interference terms are numerically small.

Explicit expressions for  $\mathcal{F}$  have been presented in [8, 9] for the  $q\bar{q}$  and  $gg$  subprocesses, excluding hadronic  $W$  decays. The complete expressions, including in hadronic  $W$  decays, are

$$\begin{aligned} \mathcal{F}_{\text{PROD}} &= c_1 \widehat{k_1 k_2} + c_2 \widehat{k_1 q_1} + c_3 \widehat{k_1 q_2} + c_4 \widehat{k_2 q_1} + c_5 \widehat{k_2 q_2} + c_6 \widehat{q_1 q_2} + c_7 \widehat{q_1 p_1} + c_8 \widehat{q_2 p_2}, \\ \mathcal{F}_{\text{DEC,tb}} &= c_7 [\widehat{q_1 q_1} + \widehat{p_1 p_1} - 2\widehat{q_1 p_1}] + c_8 [\widehat{q_2 q_2} + \widehat{p_2 p_2} - 2\widehat{q_2 p_2}], \\ \mathcal{F}_{\text{DEC,W}} &= c_9 \widehat{p_3 p_4} + c_{10} \widehat{p_5 p_6}, \\ \mathcal{F}_{\text{INT}} &= \chi_1 \left\{ c_2 [\widehat{k_1 p_1} - \widehat{k_1 q_1}] + c_4 [\widehat{k_2 p_1} - \widehat{k_2 q_1}] + c_6 [\widehat{q_2 p_1} - \widehat{q_1 q_2}] + 2c_7 [\widehat{q_1 p_1} - \widehat{q_1 q_1}] \right\} \\ &+ \chi_2 \left\{ c_3 [\widehat{k_1 p_2} - \widehat{k_1 q_2}] + c_5 [\widehat{k_2 p_2} - \widehat{k_2 q_2}] + c_6 [\widehat{q_1 p_2} - \widehat{q_1 q_2}] + 2c_8 [\widehat{q_2 p_2} - \widehat{q_2 q_2}] \right\} \\ &+ \chi_{12} c_6 [\widehat{p_1 p_2} - \widehat{q_1 p_2} - \widehat{q_2 p_1} + \widehat{q_1 q_2}], \end{aligned} \quad (7)$$

where the functions  $\widehat{pq}$  and  $\chi_i$  are defined by

$$\begin{aligned} \widehat{pq} &= \frac{p \cdot q}{p \cdot k \, q \cdot k}, \\ \chi_i &= \frac{m_t^2 \Gamma_t^2}{(q_i \cdot k)^2 + m_t^2 \Gamma_t^2} \quad (i = 1, 2), \\ \chi_{12} &= \frac{m_t^2 \Gamma_t^2 (q_1 \cdot k \, q_2 \cdot k + m_t^2 \Gamma_t^2)}{[(q_1 \cdot k)^2 + m_t^2 \Gamma_t^2] [(q_2 \cdot k)^2 + m_t^2 \Gamma_t^2]}. \end{aligned} \quad (8)$$

In terms of the gluon energy, we have  $\mathcal{F} \sim E_g^{-2}$ , and so the cross section (Eq. (4)) has the infra-red behavior  $d\sigma/dE_g \sim E_g^{-1}$ , as expected. Additional collinear singularities arise from the  $p \cdot k$  denominators when  $p^2 = 0$ .

The coefficients  $c_i$  depend on the color structure of the hard scattering and can be different for the  $q\bar{q}$  and  $gg$  processes ( $C_F = 4/3$ ,  $N = 3$ ):

| coefficient   | $q\bar{q} \rightarrow t\bar{t}$ | $gg \rightarrow t\bar{t}$ |
|---------------|---------------------------------|---------------------------|
| $c_1$         | $-\frac{1}{N}$                  | $-2C_F + 2N + 2Y$         |
| $c_2$         | $2C_F - \frac{1}{N}$            | $C_F - X - Y$             |
| $c_3$         | $\frac{2}{N}$                   | $C_F + X - Y$             |
| $c_4$         | $\frac{2}{N}$                   | $C_F + X - Y$             |
| $c_5$         | $2C_F - \frac{1}{N}$            | $C_F - X - Y$             |
| $c_6$         | $-\frac{1}{N}$                  | $2Y$                      |
| $c_7, c_8$    | $-C_F$                          | $-C_F$                    |
| $c_9, c_{10}$ | $2C_F$                          | $2C_F$                    |

Note that the coefficients  $c_7$ – $c_{10}$  are involved only in the decay contributions (including decay–decay interference) and are therefore independent of the production process. The quantities  $X$  and  $Y$  depend on the  $gg \rightarrow t\bar{t}$  subprocess energy and scattering angle. Explicit expressions and a discussion can be found in [8].

The production,  $tb$  decay, and interference contributions to  $\mathcal{F}$  have been studied in Refs. [8, 9], to which the reader is referred for further discussion. We shall focus here on the  $W$  decay contribution. Consider a single hadronically decaying  $W$ :  $W \rightarrow q\bar{q}'$ . Its most important feature, for our purposes, is that the  $W$  boson is a color singlet. Radiation from its decay products at  $O(\alpha_s)$  does not, therefore, interfere with gluons from other sources in the process. Its contribution to the radiation pattern simply adds incoherently to the total at this order.

In fact this contribution is just the familiar quark-antiquark antenna pattern, whose properties are well known and are discussed, *e.g.*, in Ref. [13]. Its color structure is the same as for the decay  $Z \rightarrow q\bar{q}$ . Here we remind the reader of a few of its properties. Because the  $q$  and  $\bar{q}$  from the  $W$  decay are taken to be massless, their contribution to  $\mathcal{F}$  depends only on their orientation relative to each other and to the gluon. Furthermore, the only other kinematical factor is an overall  $E_g^{-2}$ , which is common to all terms in  $\mathcal{F}$ . Explicitly,

$$\begin{aligned}
\mathcal{F}_{\text{DEC},W} &= 2C_F \frac{p_3 \cdot p_4}{p_3 \cdot k \, p_4 \cdot k} \\
&= 2C_F \frac{(1 - \cos \theta_{34})}{E_g^2 (1 - \cos \theta_3)(1 - \cos \theta_4)} ,
\end{aligned} \tag{9}$$

where  $\theta_3$ ,  $\theta_4$ , and  $\theta_{34}$  are, respectively, the angles between the gluon and the quark, the gluon and the antiquark, and the quark and the antiquark. Figure 1 shows the distribution given in Eq. (9) as a function of gluon angle for several  $q\bar{q}$  angles. We see the collinear singularities characteristic of radiation from massless particles. In fact most (but not all) of the radiation is concentrated in the immediate vicinity of the two

quarks, which translates in practice to strong sensitivity to jet separation cuts. We also see the string effect — the enhancement of radiation in the region between the  $q$  and  $\bar{q}$  compared to that outside them. This enhancement can be quite significant when the quarks are relatively close together in angle. As the angle increases, the enhancement decreases, but does not disappear altogether, and for quarks that are back-to-back (Fig. 1(d)) we see the plateau characteristic of initial state radiation, where the radiating particles are also back-to-back.

Finally we note that the preceding discussion of the  $W$  decay contribution to the gluon radiation is true *independent* of the source of the  $W$ , as a consequence of its being a color singlet object. In particular, although we are concerned here with hadronic top production at the Fermilab Tevatron collider, hadronic  $W$  decays in top production at, for example, an  $e^+e^-$  collider, are taken into account in exactly the same way. At the order to which we are working, the  $W$  decay antenna simply adds incoherently to the contribution from the remaining sources of gluon radiation in any process of interest.<sup>3</sup>

### 3 Gluon distributions in $t\bar{t}$ events at the Tevatron

#### 3.1 Single hadronic $W$ decay: lepton + jets mode

The soft gluon radiation pattern described by Eq. (4) can be combined with the lowest-order cross section to obtain the full gluon distribution in a particular experimental situation. In this section we present the resulting gluon distributions for  $t\bar{t}$  production at the Fermilab Tevatron  $p\bar{p}$  collider for the case where one  $W$  decays leptonically and the other decays hadronically, *i.e.*, the ‘lepton + jets’ mode. As we have seen in the previous section, the contribution from the hadronic  $W$  decay adds incoherently to the other contributions. The latter correspond to what we would have for the dilepton mode, *i.e.*, to the results in Ref. [9]. We note that results for the production and ‘ $tb$ ’ decay distributions presented below are virtually the same as in [9], where a more complete discussion of them can be found. Our emphasis here will be on the new features resulting from the  $W$  decay contribution.

We consider the process  $p\bar{p} \rightarrow t\bar{t} \rightarrow b l \nu \bar{b} q \bar{q}$ , with gluons generated according to Eq. (4), with  $c_{10} = 0$  in Eq. (7), for  $p\bar{p}$  center-of-mass energy 1.8 TeV. We take  $m_t = 174 \text{ GeV}/c^2$ ,  $M_W = 80 \text{ GeV}/c^2$ , and  $m_b = 5 \text{ GeV}/c^2$  and we use MRS(A') parton distributions [16]. We work at the parton level, with kinematic cuts corresponding

---

<sup>3</sup>Perturbative interference between radiation off the  $W$  and other colored particles in the scattering process begins at  $O(\alpha_s^2)$  with the exchange of two gluons in a color singlet state. This has been studied in the context of  $e^+e^- \rightarrow W^+W^- \rightarrow q\bar{q}q\bar{q}$  production [14, 15]. In general, such interference is suppressed by factors of  $1/N_c^2$  and  $(\Gamma_W/\omega)^2$ , where  $\omega$  is a scale characteristic of the gluon energies, and is therefore numerically very small [15].

roughly to those in the experiments: central production of leptons and quarks, some minimum separation of jets from each other and from the lepton, and energy and transverse momentum cuts appropriate to detectability of jets but also consistent with the soft gluon approximation. The cuts are

$$\begin{aligned}
|\eta_i| &\leq 1.5, \\
|\eta_g| &\leq 3.5, \\
10 \text{ GeV}/c &\leq p_T^g \leq 25 \text{ GeV}/c, \\
E_g &\leq 50 \text{ GeV}, \\
10 \text{ GeV}/c &\leq p_T^i, \\
\Delta R_{ig}, \Delta R_{ij} &\geq 0.5,
\end{aligned} \tag{10}$$

where  $\eta$  is the pseudorapidity and  $(\Delta R)^2 = (\Delta\eta)^2 + (\Delta\phi)^2$ . In Eq. (10)  $g$  represents the gluon jet and  $i$  and  $j$  represent any other detected jet ( $b$ ,  $\bar{b}$ , or either of the quarks from the  $W$  decay) or the charged lepton. The  $\eta_g$  and  $\Delta R_{ig}$  cuts eliminate the collinear singularities associated with emission from massless particles.

The resulting distributions in the gluon energy and transverse momentum are shown as solid histograms in Fig. 2. The contribution associated with top production is shown as a dotted line, that for  $\mathcal{F}_{\text{DEC},tb}$  as a dashed line, and that for  $\mathcal{F}_{\text{DEC},W}$  as a dot-dashed line. (Interference terms are included in the total but are too small to appear on the plots.) From the figure we see two features of the  $W$  decay contribution that will also appear in the rapidity distribution, *viz.*, that it is comparable in both size and shape to the remaining decay piece. Recall that the latter comes from the decays of both the  $t$  and the  $\bar{t}$ , whereas the former involves only the decay of a single top.

The gluon pseudorapidity distribution is shown in Fig. 3; again the  $W$  decay piece looks very similar to the ‘ $tb$ ’ piece. We conclude that hadronic  $W$  decays contribute substantially to gluon radiation in the central rapidity region, more than doubling the amount of radiation associated with the top quark decays.

For purposes of distinguishing the production and decay contributions in the dilepton case, we also considered in [9] the behavior of the gluon distribution as a function of angular distance  $\Delta R_{bg}$  of the gluon from the  $b$  quark. In Fig. 4(a) we show the distribution in  $\Delta R_{bg}$  for very small angles ( $\Delta R < 0.5$ ). Except for allowing  $\Delta R_{bg} \geq 0.01$ , we have retained the cuts specified in Eq. (10). We see that in this region the distribution is dominated by the ‘ $tb$ ’ decay contribution (dashed histogram) and that as  $\Delta R$  decreases, the distribution increases and then turns over, displaying the ‘dead-cone’ behavior characteristic of radiation from massive particles [13]. In contrast, the distribution in the angular distance  $\Delta R_{Wjet,g}$  between the gluon and one of the (massless) quarks from the hadronic  $W$  decay, shown in Fig. 4(b), should have a singularity when the quark and gluon are collinear. We see that when we reduce the minimum allowed

$\Delta R_{Wjet,g}$  to 0.01, the distribution shows no signs of turning over at small angles. The singularity is avoided only by the  $\Delta R$  cut.

While it is true that Fig. 4 shows the difference between emissions from massless and massive particles, the effect occurs at angles much too small for the difference to be detected experimentally. A less academic view appears in Fig. 5(a) and (b), where we look at the same distributions on a larger scale after reimposing the  $\Delta R > 0.5$  requirement. The distributions look remarkably similar, the only real difference being which contribution dominates at small angles: the ‘ $tb$ ’ contribution (dashed histogram) in Fig. 5(a) and the  $W$  decay contribution (dot-dashed histogram) in Fig. 5(b). This could be used in principle to distinguish between the two decay contributions if one knew, from secondary vertex detection, for example, which were the  $b$  jets and which were those from the  $W$  decays (assuming the gluon jet to be the softest one). However the results are quite sensitive to both the  $\Delta R$  cuts and to fragmentation, which is not included in our parton-level analysis.

A perhaps more promising way to separate out the  $W$  decay contribution is to note that it is associated with only *one* of the top decays. If the top quarks are produced more or less back-to-back, then some of that separation can be expected to survive the decay process. In that case the charged lepton would tend not to be too close to the quarks from the other  $W$  decay. And since gluons prefer to be near the quarks that radiated them, radiation from the hadronic  $W$  decay should increase with angular distance from the charged lepton. The expected effect is quantified in Fig. 6, where we show the gluon distribution as a function of the azimuthal angle difference between the lepton and the gluon. We consider the azimuthal angles because the  $t$  and  $\bar{t}$  are produced back-to-back in the transverse plane. In addition to the cuts of Eq. (10), we require the angular separation of the  $b$  and  $\bar{b}$  to be greater than  $45^\circ$ , and that all detected particles (lepton and all jets, including the soft gluon jet) have  $|\eta| < 1$ . These additional cuts are designed to increase the likelihood that the event is more central and the  $t$  decay products more widely separated from those of the  $\bar{t}$ . The pseudorapidity cut on the gluon has the added advantage that it eliminates a large portion of the contribution from production (*cf.* Fig. 3). In Fig. 6 we see the expected behavior. All of the distributions are suppressed below about  $30^\circ$  because of the  $\Delta R$  cut. Beyond that, the production and ‘ $tb$ ’ decay contributions are relatively flat. In contrast, the  $W$  decay contribution (dot-dashed histogram) starts out at about the same size as the other two and increases with increasing angle, reaching a maximum about 50% higher than the initial value. *All* of the increase in the total gluon distribution is due to the increase in the  $W$  decay contribution.

Similar effects would be expected in the distribution in azimuthal angle difference between the gluon and one of the  $b$  quarks, due to the typical angular separation of about  $\pi/2$  between the  $b$  and  $W$  from a single top decay. However, using the lepton is



more practical experimentally because there is only one lepton in each event,<sup>4</sup> and also because identifying it and measuring its momentum does not involve the complications associated with doing so for jets.

### 3.2 Two hadronic $W$ decays: all jets mode

If both the  $W^+$  and  $W^-$  in a  $t\bar{t}$  event decay hadronically, then there are six jets in the final state at leading order. The advantages of this mode are its large branching ratio and the fact that, in principle, both the  $t$  and  $\bar{t}$  can be fully reconstructed from their decay jets. In practice, combinatorics and huge QCD backgrounds make this task more difficult. In addition, radiation of a gluon can give rise to an extra jet, further complicating matters.

If the additional gluon is soft, its distribution is given by Eq. (4) with the coefficient  $c_{10} = 2C_F$  in  $\mathcal{F}_{\text{DEC},W}$  as given in the table. Now, in addition to the  $W^+$  decay contribution discussed above, we also have one from the hadronic decay of the  $W^-$ . This new contribution is the same as that from the  $W^+$ , and it adds incoherently. Therefore radiation from the  $W$  decays is effectively doubled when both  $W$ 's decay to quarks. This is illustrated in Fig. 7, which shows the gluon rapidity distribution at the Tevatron, where both  $W$ 's contribute to the  $W$  decay piece (shown as a dot-dashed histogram). The cuts are as in Eq. (10). Their effect here is slightly different from above, however, because now there is no charged lepton, and the lepton and neutrino (to which no cuts were applied previously) are replaced by two quarks. The jet cuts now apply to *all* of the particles in the final state. This accounts for the fact that the  $W$  decay contribution in the all jets case is slightly less than twice that for lepton + jets. The transverse momentum, energy, and  $\Delta R$  distributions exhibit a similar doubling of the  $W$  decay contribution, and are omitted for brevity.

### 3.3 Expectations for the LHC

The CERN Large Hadron Collider (LHC) will produce large numbers of top quark pairs. Gluon radiation in top production and decay at the LHC differs from that at the Tevatron largely because of the difference in collision energies. At the higher-energy LHC, the top quarks are more energetic, and the cross section is dominated by the gluon-gluon initial state, in contrast to the quark-antiquark annihilation that dominates at the Tevatron. The result [17] is a much larger proportion of production-stage radiation at the LHC than the Tevatron, with relatively little (on the order of 10–20%) radiation occurring in the decays in the dilepton case. We expect the effects of radiation from hadronic  $W$  decays to be similar to effects at the Tevatron:

---

<sup>4</sup>Not counting those from semileptonic  $b$  decays, which can presumably be eliminated with an isolation cut.

radiation from a single hadronically decaying  $W$  would be comparable to the total decay contributions from the  $tb$  and  $\bar{t}\bar{b}$  antennae. Production-stage radiation would continue to dominate. We defer a detailed discussion to an exact treatment.

## 4 Conclusions

We have presented results for soft gluon radiation in top quark production and decay at the Fermilab Tevatron for the cases relevant for direct reconstruction of the top quarks: the lepton + jets and all jets decay modes. Allowing for radiation at  $O(\alpha_s)$  from hadronic  $W$  decays is straightforward because the  $W$  is a color singlet. The corresponding contribution simply adds incoherently to the total, with no interference with the remaining contributions. For this reason, soft radiation in  $W$  decays is also easily treated in top production in  $e^+e^-$  collisions by adding  $\mathcal{F}_{\text{DEC},W}$  to the  $\mathcal{F}$  appropriate to the electron-positron initial state (*cf.* Eqs. (4,5)).

We found that, at the Tevatron, gluons radiated in hadronic  $W$  decays contribute substantially to the total amount of radiation in the central region. In particular, gluon radiation from *each* hadronic  $W$  decay is comparable both in size and distribution to the *total*  $tb$  and  $\bar{t}\bar{b}$  decay contributions. The  $W$  and non- $W$  contributions are thus difficult to distinguish. But by considering the distribution in the azimuthal angle between the gluon and the charged lepton in the lepton + jets mode we saw that some separation is possible. We also note that since the  $tb$  and  $\bar{t}\bar{b}$  decay contributions comprise the total decay contribution in the dilepton detection mode, the  $W$  decay contribution could in principle be isolated by making a direct comparison of jet distributions in dilepton and lepton + jets events.

In attempts to measure the top mass by reconstructing the momenta of its decay products, it is very important to take into account the presence of extra jets due to gluon radiation. As we have shown in the soft approximation, hadronic  $W$  decays give rise to significant amounts of gluon radiation. An analysis of the impact of this radiation on top momentum reconstruction requires an exact treatment, which we plan in future work.

## Acknowledgements

This work was supported in part by the U.S. Department of Energy, under grant DE-FG02-91ER40685, and by the University of Rochester SummerReach Program.

## References

- [1] CDF collaboration: F. Abe *et al.*, Phys. Rev. Lett. **74** (1995) 2626.

- [2] DØ collaboration: S. Abachi *et al.*, Phys. Rev. Lett. **74** (1995) 2632.
- [3] G. Jikia, Phys. Lett. **257B** (1991) 196.
- [4] V.A. Khoze, L.H. Orr and W.J. Stirling, Nucl. Phys. **B378** (1992) 413.
- [5] Yu.L. Dokshitzer, V.A. Khoze, L.H. Orr and W.J. Stirling, Nucl. Phys. **B403** (1993) 65.
- [6] C.R. Schmidt, hep-ph/9504434, Phys. Rev. **D54** (1996), in press.
- [7] L.H. Orr, T. Stelzer, and W.J. Stirling, Phys. Lett. **B354** (1995) 442.
- [8] V.A. Khoze, J. Ohnemus and W.J. Stirling, Phys. Rev. **D49** (1994) 1237.
- [9] L.H. Orr and W.J. Stirling, Phys. Rev. **D51** (1995) 1077.
- [10] B. Lampe, Phys. Lett. **B348** (1995) 196.
- [11] L.H. Orr, T. Stelzer and W.J. Stirling, Phys. Rev. **D52** (1995) 124; Phys. Lett. **B354** (1995) 442.
- [12] V. Barger, P.G. Mercadante and R.N.J. Phillips, Phys. Lett. **B371** (1996) 117.
- [13] Yu.L. Dokshitzer, V.A. Khoze, A.H. Mueller and S.I. Troyan, *Basics of Perturbative QCD*, Editions Frontieres, 1991.
- [14] G. Gustafson, U. Pettersson and P. Zerwas, Phys. Lett. **B209** (1988) 90.
- [15] T. Sjöstrand and V.A. Khoze, Z. Phys. **C62** (1994) 281; Phys. Rev. Lett. **72** (1994) 28.
- [16] A.D. Martin, R.G. Roberts and W.J. Stirling, Phys. Lett. **B354** (1995) 155.
- [17] L.H. Orr, T. Stelzer and W.J. Stirling, in preparation.

## Figure Captions

- [1] Single  $W$  decay contribution  $\mathcal{F}_{\text{DEC}}$  (Eq. (9)) to the soft gluon radiation pattern in the  $\theta - \phi$  plane, in arbitrary units, for  $\theta_{34} =$  (a)  $45^\circ$ , (b)  $90^\circ$ , (c)  $135^\circ$ , and (d)  $180^\circ$ .

- [2] Distributions in (a) the gluon energy and (b) the gluon transverse momentum, in  $t\bar{t}$  production, via the subprocesses  $q\bar{q}, gg \rightarrow bW^+\bar{b}W^-$ , in  $p\bar{p}$  collisions at  $\sqrt{s} = 1.8$  TeV, with  $W^+ \rightarrow q\bar{q}$ . Contributions from production (dotted lines),  $\mathcal{F}_{\text{DEC, tb}}$  decay (dashed lines), and  $\mathcal{F}_{\text{DEC, W}}$  (dot-dashed lines) are shown along with their totals (solid lines). The cuts are listed in Eq. (10).
- [3] Gluon pseudorapidity distributions in  $t\bar{t}$  production, via the subprocesses  $q\bar{q}, gg \rightarrow bW^+\bar{b}W^-$ , in  $p\bar{p}$  collisions at  $\sqrt{s} = 1.8$  TeV, with  $W^+ \rightarrow q\bar{q}$ . The net distribution is shown as a solid line; contributions from production (dotted lines),  $\mathcal{F}_{\text{DEC, tb}}$  decay (dashed lines), and  $\mathcal{F}_{\text{DEC, W}}$  (dot-dashed lines) are also shown. The cuts are listed in Eq. (10).
- [4] Distribution in  $\Delta R$  between the gluon and (a) the  $b$  quark and (b) the charged lepton. Cuts are as in Eq. (10), except for allowing (a)  $\Delta R_{bg} \geq 0.01$  and (b)  $\Delta R_{Wjet, g} \geq 0.01$ .
- [5] Distribution in  $\Delta R$  between the gluon and (a) the  $b$  quark and (b) the charged lepton. The cuts are as in Eq. (10).
- [6] Distribution in the azimuthal angle between the charged lepton and gluon jet. The cuts are as in Eq. (10), except  $|\eta| < 1$  for all detected particles and the angle between the  $b$  and  $\bar{b}$  must be greater than  $45^\circ$ .
- [7] Gluon pseudorapidity distributions in  $t\bar{t}$  production, via the subprocesses  $q\bar{q}, gg \rightarrow bW^+\bar{b}W^-$ , in  $p\bar{p}$  collisions at  $\sqrt{s} = 1.8$  TeV, with both  $W$ 's decaying hadronically. The net distribution is shown as a solid line; contributions from production (dotted lines),  $\mathcal{F}_{\text{DEC, tb}}$  decay (dashed lines), and  $\mathcal{F}_{\text{DEC, W}}$  (dot-dashed lines) are also shown. The cuts are listed in Eq. (10).

This figure "fig1-1.png" is available in "png" format from:

<http://arxiv.org/ps/hep-ph/9605369v1>

This figure "fig1-2.png" is available in "png" format from:

<http://arxiv.org/ps/hep-ph/9605369v1>

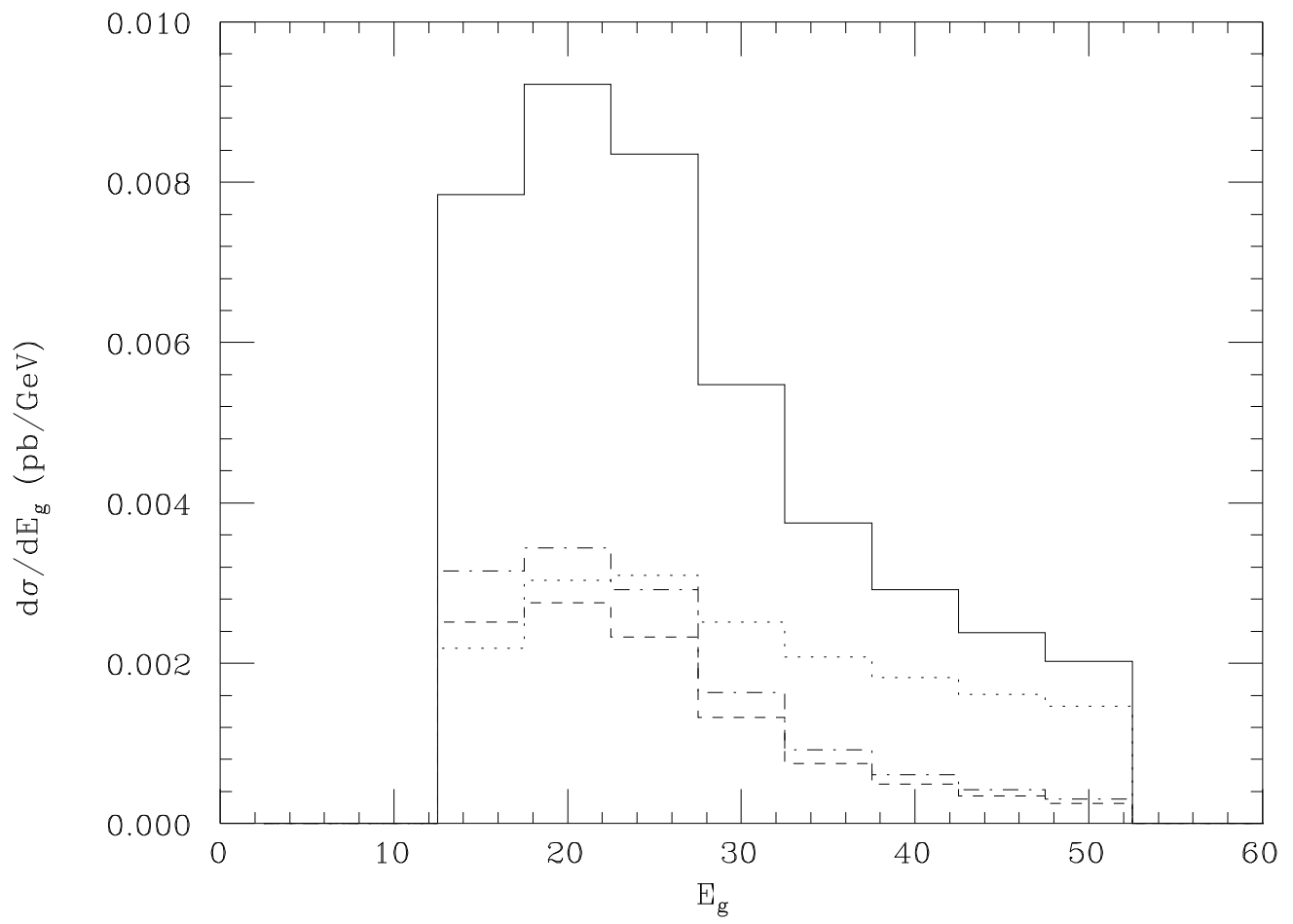


Figure 2(a)

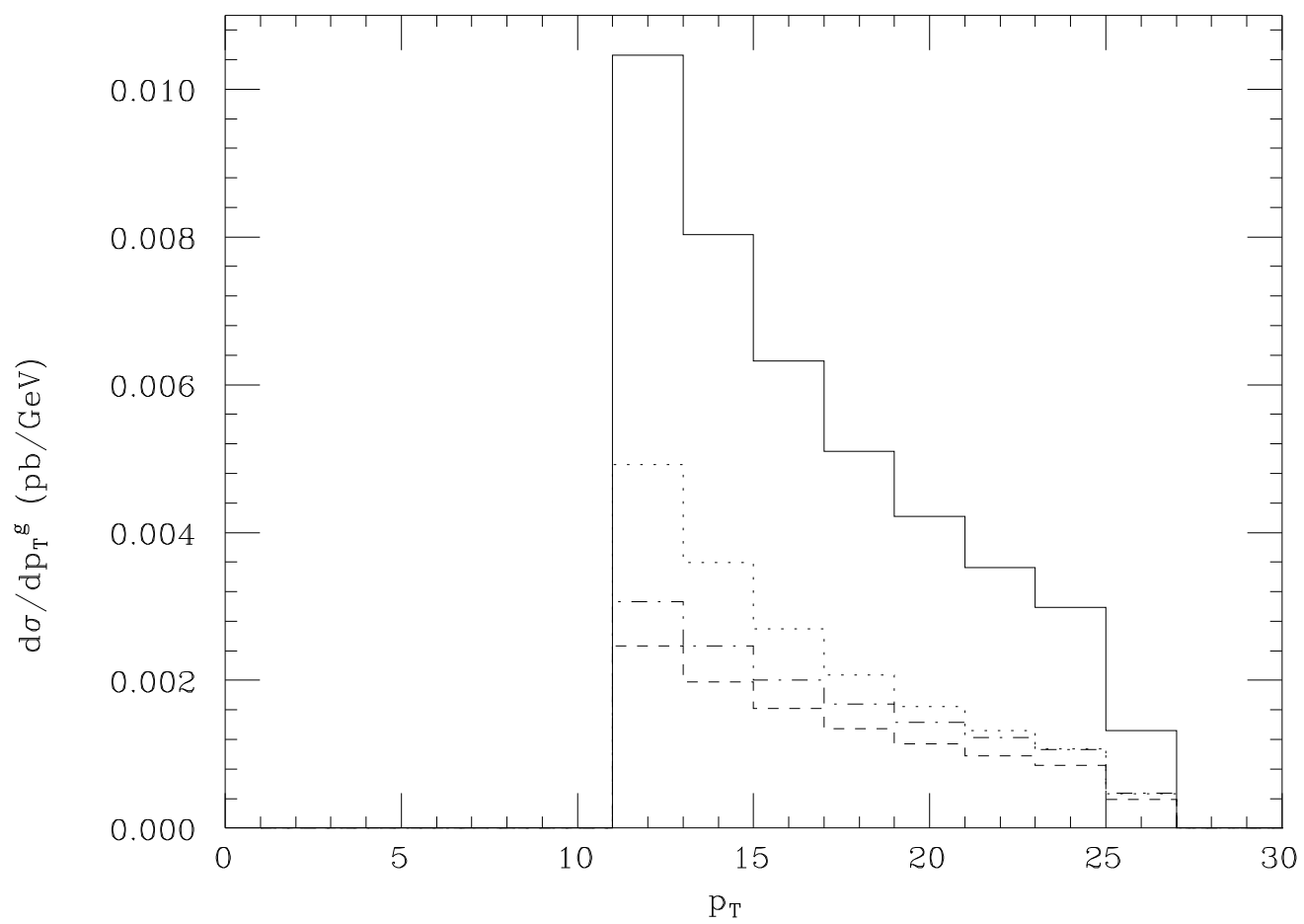


Figure 2(b)



This figure "fig1-3.png" is available in "png" format from:

<http://arxiv.org/ps/hep-ph/9605369v1>

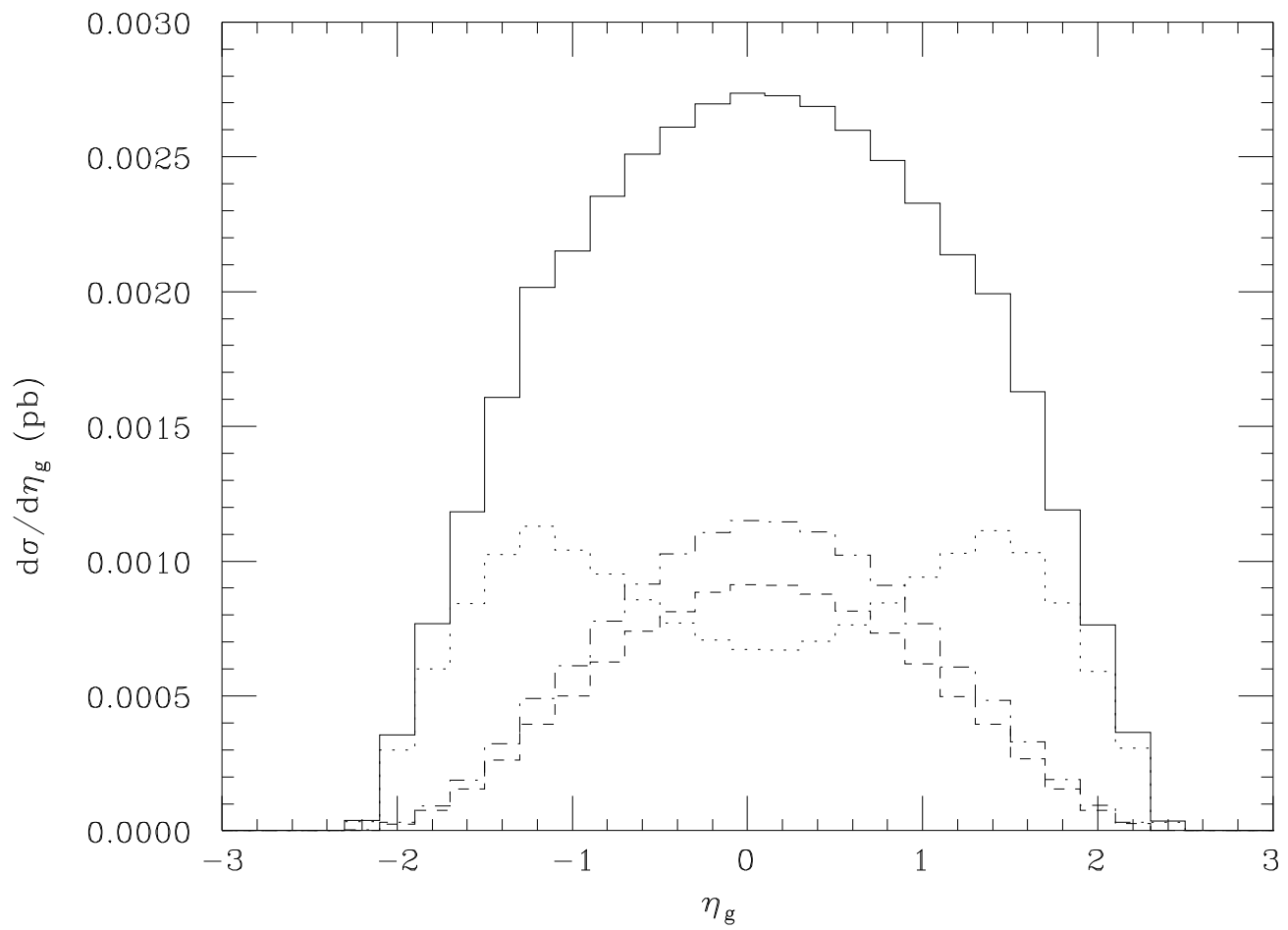


Figure 3

This figure "fig1-4.png" is available in "png" format from:

<http://arxiv.org/ps/hep-ph/9605369v1>

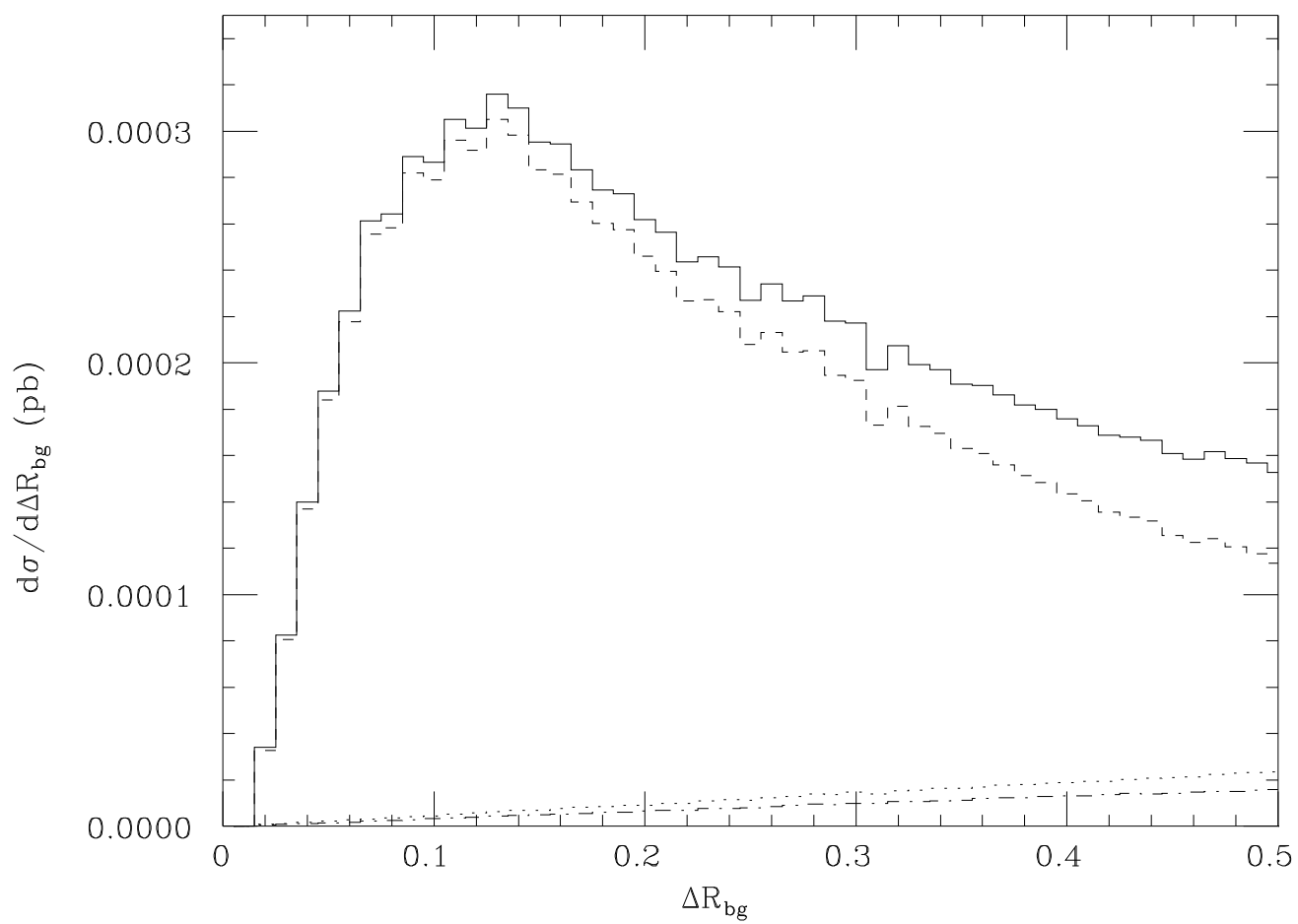


Figure 4(a)

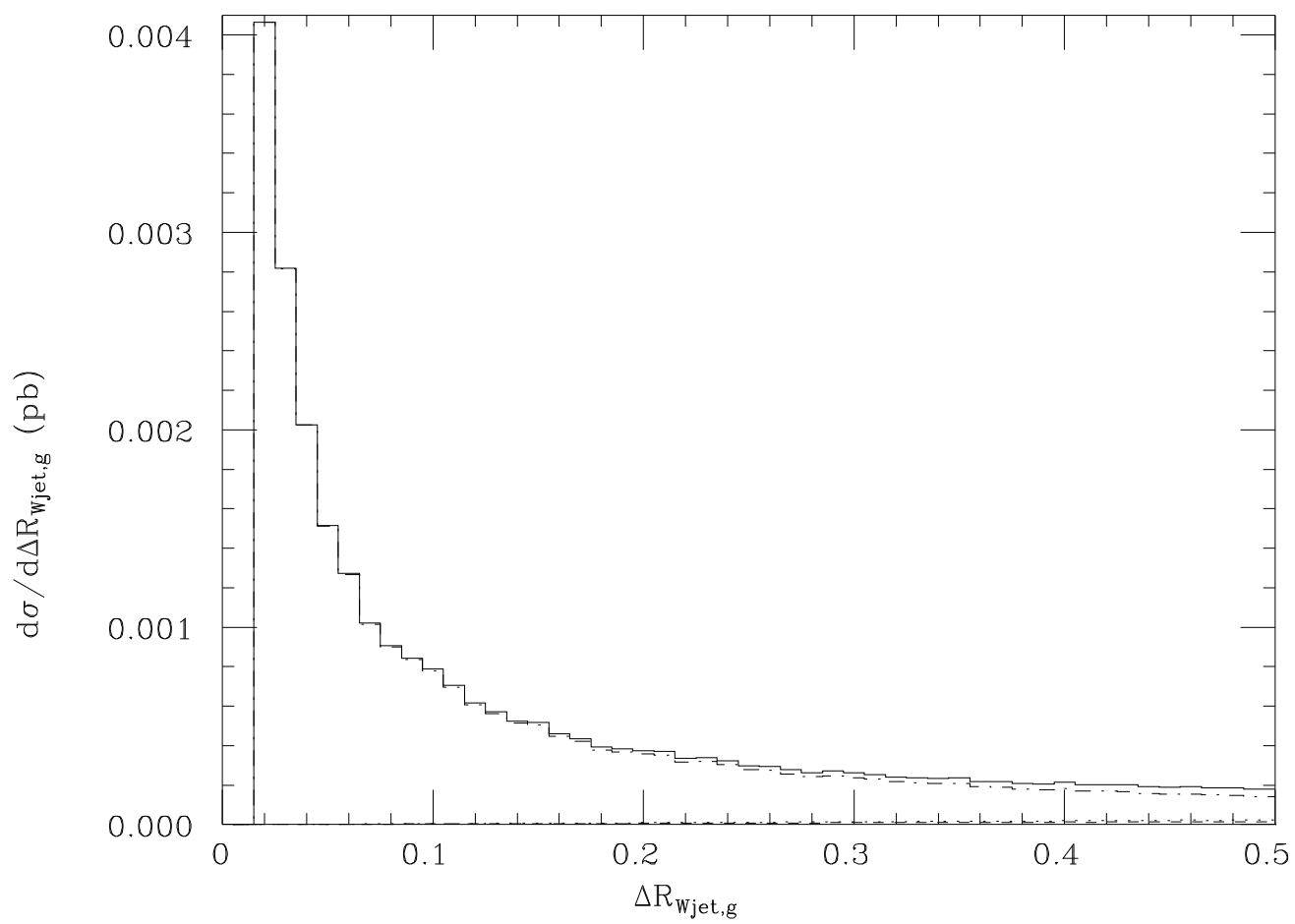


Figure 4(b)

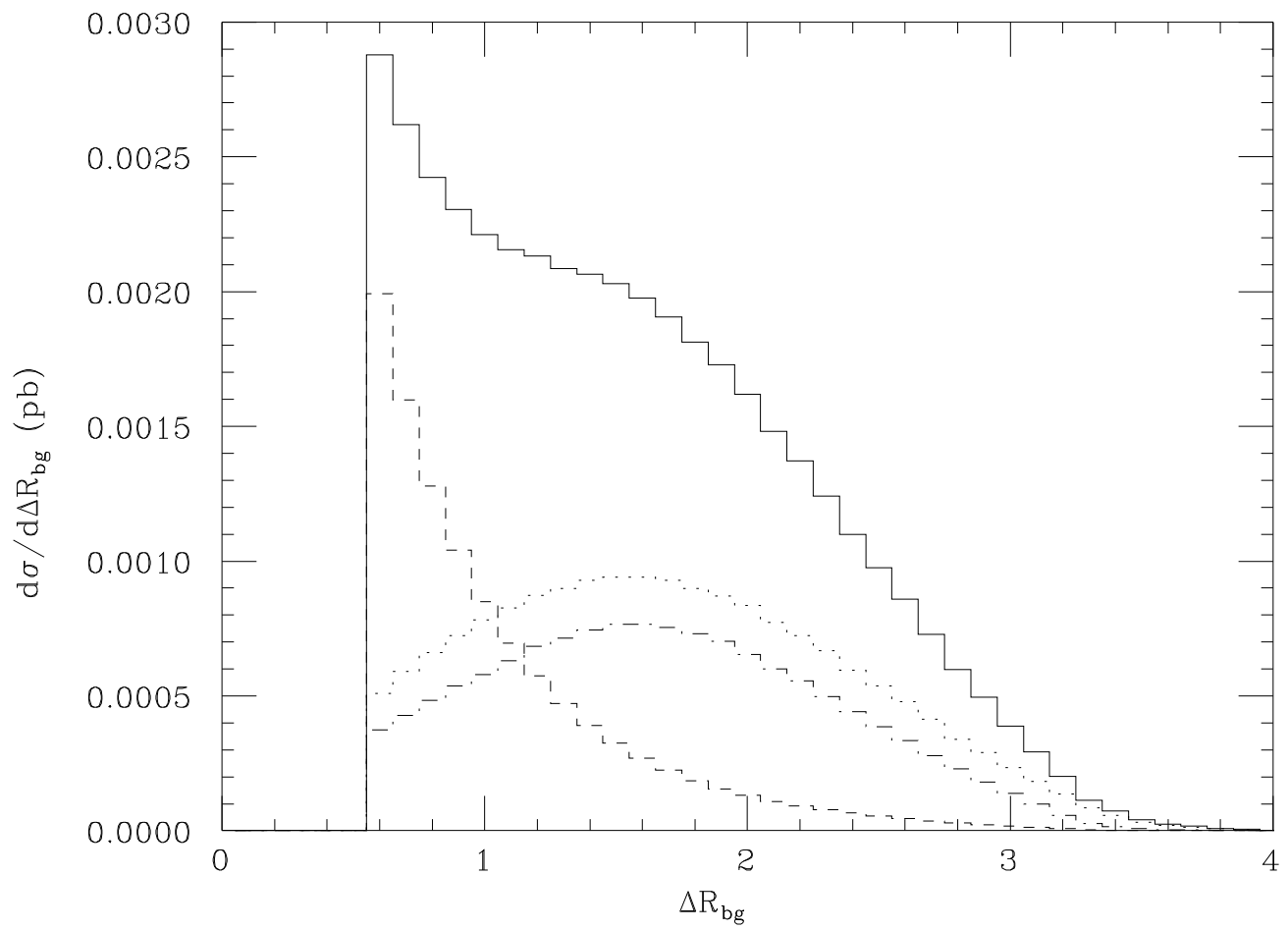


Figure 5(a)

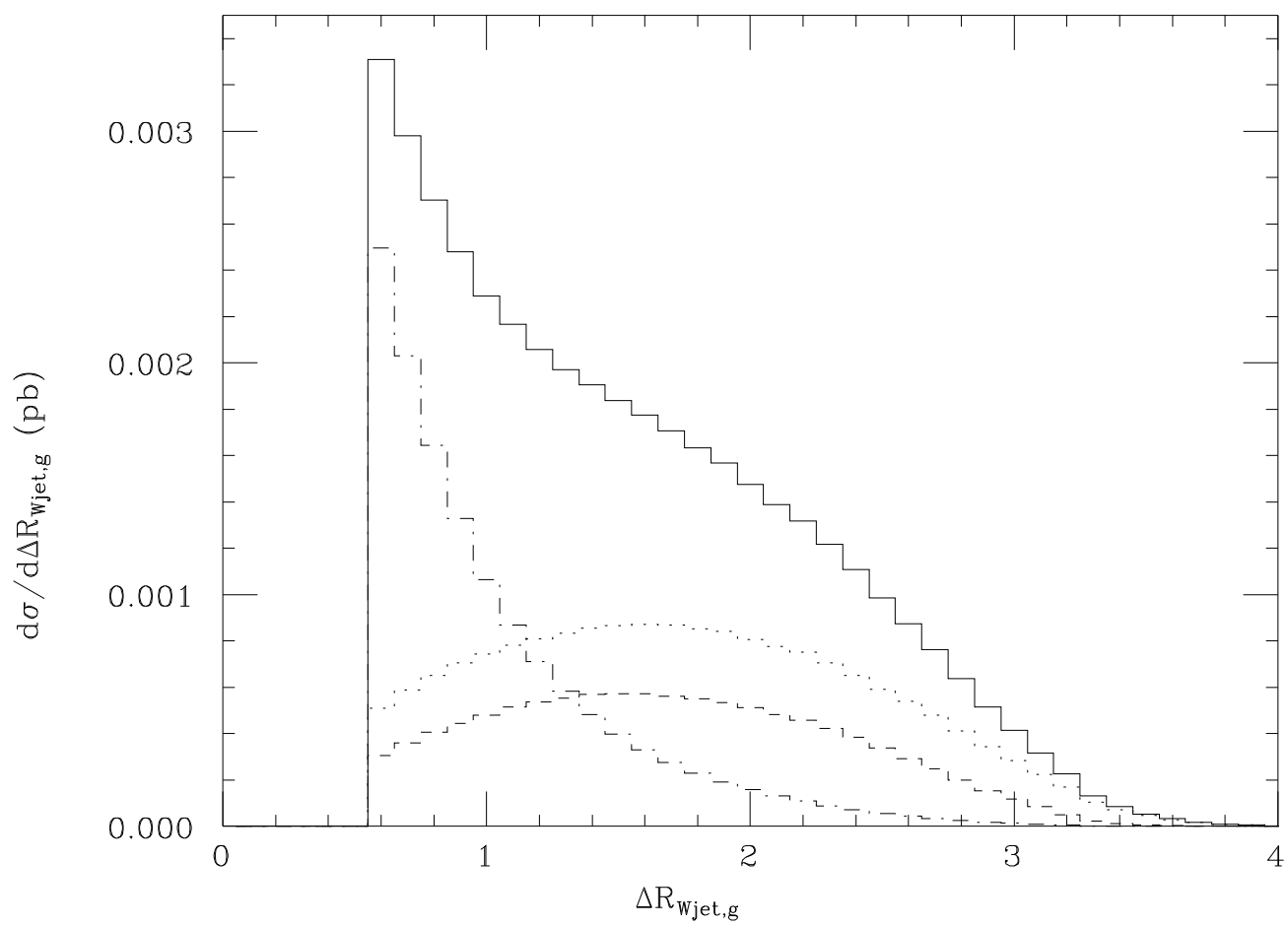


Figure 5(b)

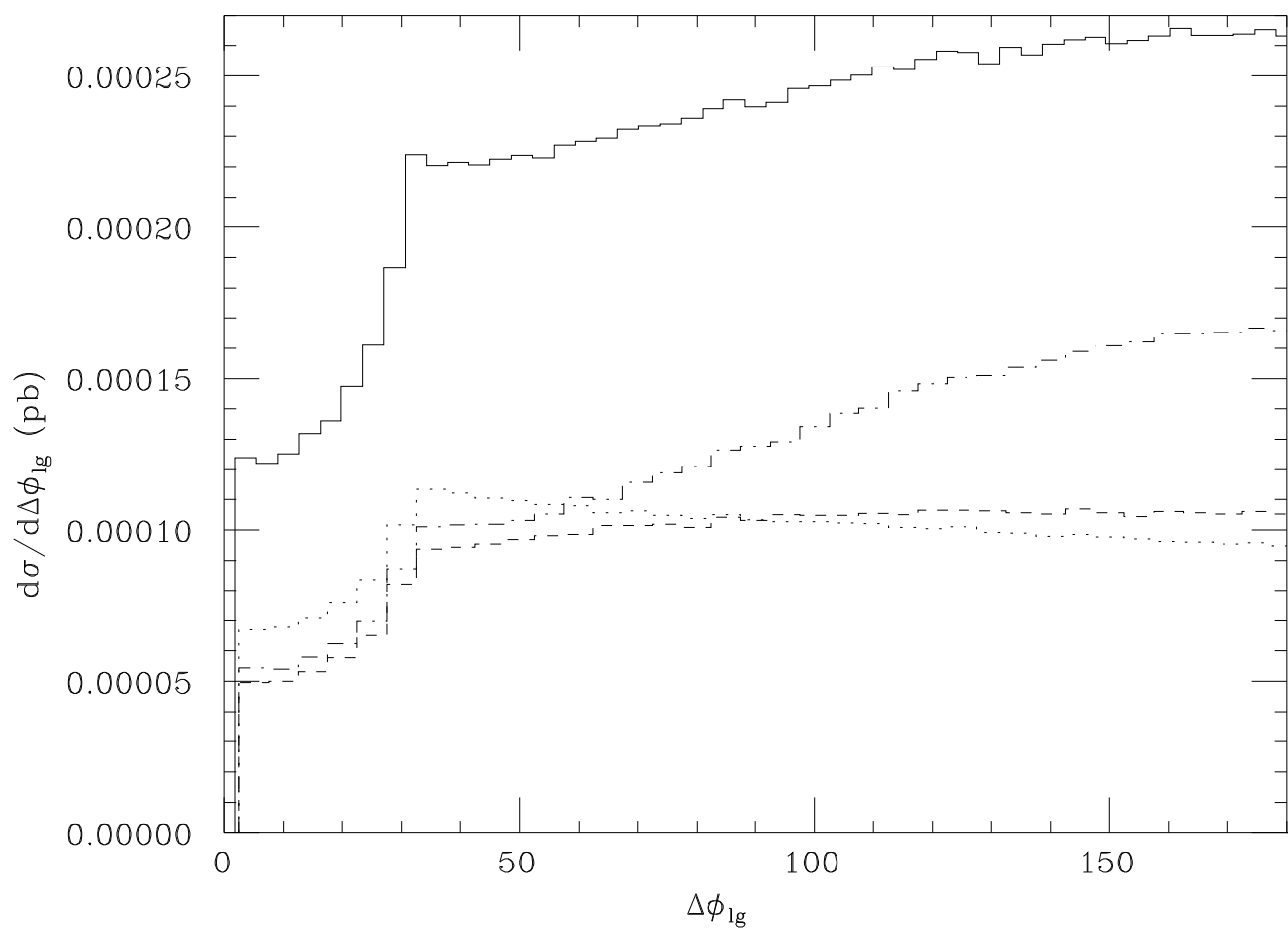


Figure 6



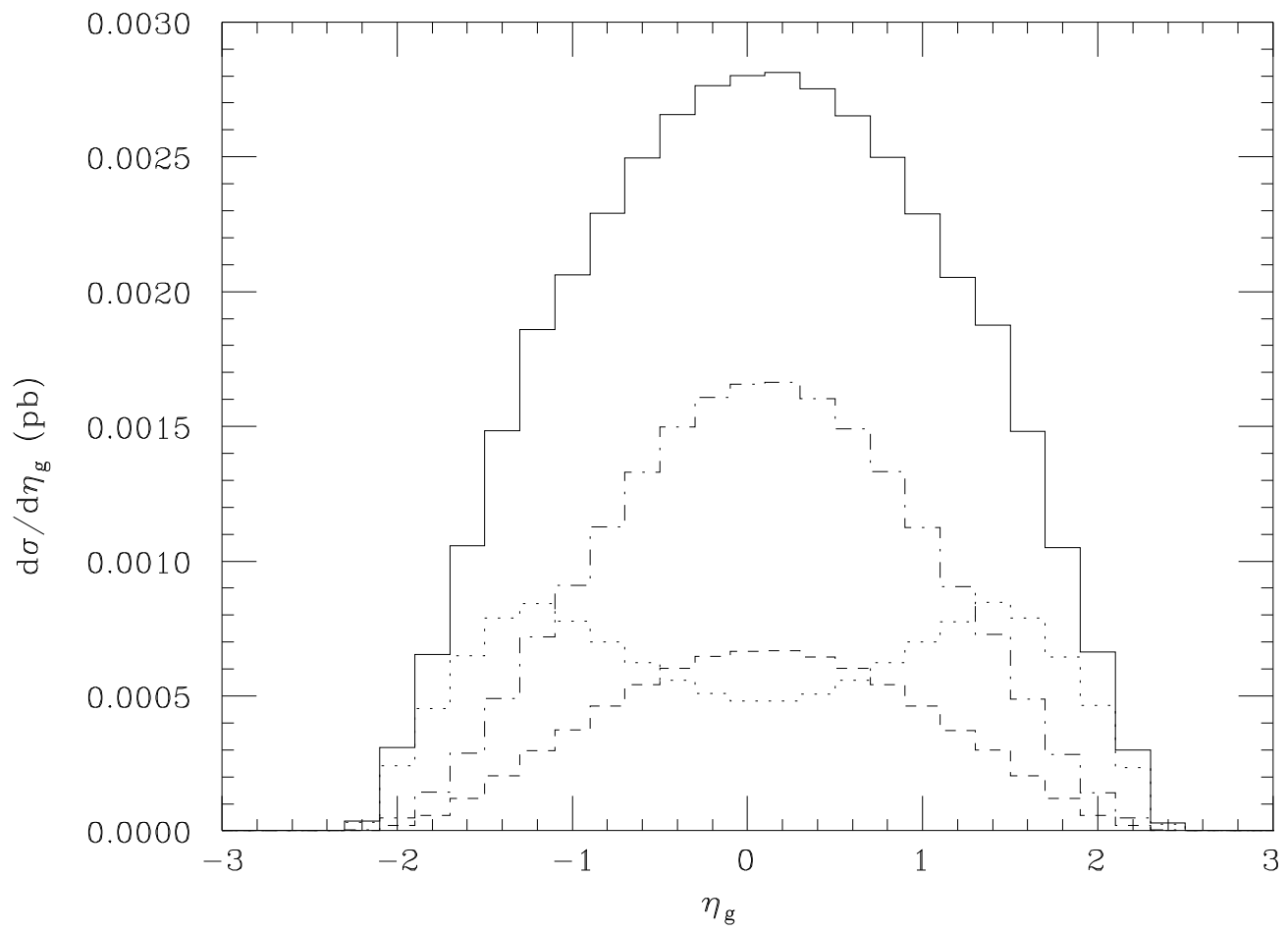


Figure 7